

Achiral Single Molecule Magnet and Chiral Single Chain Magnet

Norihisa Hoshino, Yoshihiro Sekine, Masayuki Nihei, and Hiroki Oshio*

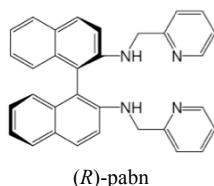
Received (in XXX, XXX) Xth XXXXXXXXXX 200X, Accepted Xth XXXXXXXXXX 200X

First published on the web Xth XXXXXXXXXX 200X

DOI: 10.1039/b000000x

Achiral molecular square and chiral chain composed of cyanide bridged Fe^{III} and Ni^{II} ions were prepared, and they act as single molecule magnet and chiral single chain magnet, respectively.

Chiral compounds are an important class of materials and they have been attached intense current research interests in the field of asymmetric catalysis, non-linear optics, and ferroelectrics.¹ In the field of magnetic materials, the combination of ferromagnetism and chirality can result in magneto-chiral dichroism (MChD)² and chiral magneto-structural effects,³ which can be applied to magneto-optical multifunctional materials. Recently, dielectric relaxation and second harmonic generation (SHG) were, respectively, observed in molecule based chiral single chain magnets (SCMs).^{4,5} Single molecule magnets (SMMs)⁶ and SCMs⁷ are single domain magnets below their critical temperatures, and the former show quantum tunnelling of magnetization (QTM). Although SCMs with chiral spin centers are expected to show enhanced synergistic effects of chirality and magnetism, the number of chiral SCMs is still limited. We report here that the reaction of a racemic mixture and homo-chiral of Ni²⁺ complexes with [Fe^{III}(tp)(CN)₃]⁻ yielded a cyanide bridged achiral SMM of the formula [Fe^{III}₂Ni^{II}₂(CN)₆(tp)₂((R)-pabn)((S)-pabn)](PF₆)₂·2H₂O·4CH₃CN (**1**) and a chiral SCM of *catena*-[Ni^{II}((R)-pabn)][Fe^{III}(tp)(CN)₃]PF₆·2MeOH (**2**) ((R) and (S)-pabn = (R) and (S)-N2,N2'-bis(pyridin-2-ylmethyl)-1,1'-binaphthyl-2,2'-diamine, and Htp = hydrotris(pyrazolyl)borate, respectively).



The chiral ligands, (R) and (S)-pabn, were synthesized following literature methods.⁸ The reactions of a racemic mixture of [Ni^{II}(pabn)Cl₂] and a chiral [Ni^{II}((R)-pabn)Cl₂] with (Bu₄N)₂[Fe^{III}(CN)₃(tp)]⁹ and (Bu₄N)PF₆ yielded cyanide bridged discrete and chain systems of **1** and **2** as brown tablets and brown needles, respectively. **1** crystallizes in the triclinic space group of *P*1 and **2** crystallizes in the chiral space group

of *P*2₁2₁2₁ with a Flack's parameter of 0.01(1) for the present structure (Figure 1). Ligands tp⁻ and (R or S)-pabn act as tri- and tetra-dentate ligands, respectively, both in **1** and **2**. The iron ions in **1** and **2** are in the trivalent low spin states, as determined by charge balance and coordination bond lengths.

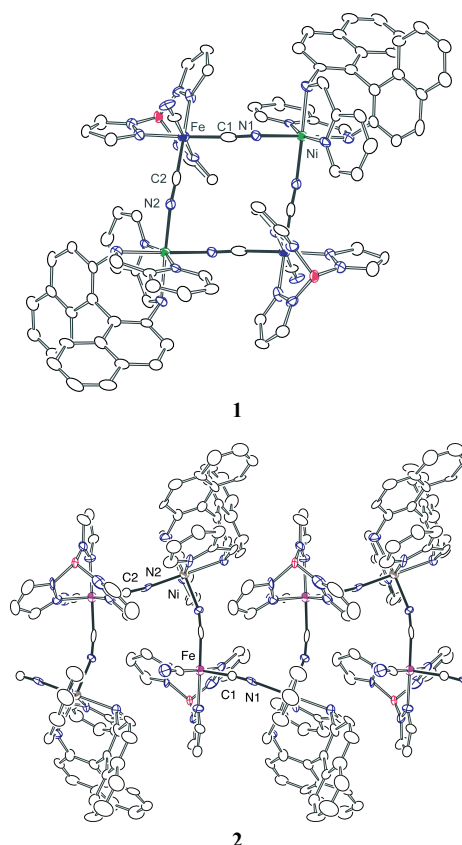


Fig. 1 ORTEP diagram of **1**²⁺ (top) and **2**⁺ (bottom). Selected bond lengths for **1**: Fe(1)-C(1) 1.946(13), Fe(1)-C(2) 1.925(12), Fe(1)-C(3) 1.921(12), Ni(1)-N(1) 2.078(9), Ni(1)-N(2) 2.093(9), and for **2**: Fe(1)-C(1) 1.934(4), Fe(1)-C(2) 1.906(4), Fe(1)-C(3) 1.922(4), Ni(1)-N(1) 2.067(3), Ni(1)-N(2) 2.042(3).

Mössbauer parameters (relative to metallic iron) at 20 K are (δ = 0.019(3) mm s⁻¹ and Δ = 1.06(1) mm s⁻¹) for **1** and (δ = 0.012(1) mm s⁻¹ and Δ = 1.39(1) mm s⁻¹) for **2**, and the parameters are in agreement with the assignments. **1**²⁺ locates on the crystallographic center of inversion and the square shaped cation is composed of cyanide bridged [Ni^{II}((R)-pabn)]²⁺, [Ni^{II}((S)-pabn)]²⁺, and two [Fe^{III}(CN)₃(tp)]⁻ components. The six coordination sites of the Fe^{III} ions are filled with three nitrogen donor atoms from the tp⁻ ligand and three carbon atoms from the CN⁻ ions, where two cyanide

Graduate School of Pure and Applied Sciences, University of Tsukuba, Tennodai 1-1-1, Tsukuba 305-8571 Fax: +81-29-853-4238; Tel: +81-29-853-4238; E-mail: oshio@chem.tsukuba.ac.jp

† Electronic Supplementary Information (ESI) available: Fig. S1 and S2, and Table S1 and S2. CCDC 756081 (**1**) and 756082 (**2**). For ESI and crystallographic data in CIF or other electronic format see DOI: 10.1039/b000000x/

nitrogen atoms of the CN⁻ ions bridge to the Ni^{II} ions. The coordination bond lengths of Fe-C(cyanide) are in the range of 1.921(12) - 1.946(13) Å, and those of Fe-N bonds are 1.963(9) - 1.982(9) Å, which are characteristic of low-spin Fe^{III} ions. The Ni^{II} ions have a distorted octahedral coordination geometry, of which the *cis* positions are occupied by cyanide nitrogen atoms and the remaining four sites are coordinated by (*R*)- or (*S*)-pabn. Therefore, the two Ni^{II} ions in the square have Δ and Λ configurations, respectively. The Ni-N coordination bond lengths are 2.078(9) - 2.093(9) Å and 2.087(9) - 2.183(8) Å for the cyanide ions and pabn, respectively.

2⁺ has a chiral 1D structure in which Fe^{III} and Ni^{II} ions are alternately bridged by cyanide ions. The coordination environments about the Fe^{III} and Ni^{II} ions in **2** are very similar to those in **1**, except that the Ni^{II} ions are coordinated by only (*R*)-pabn in addition to the two cyanide groups, hence, they have the Λ configuration. The six coordination sites of the Fe^{III} ion are occupied by three nitrogen and three carbon atoms from tp⁻ and cyanide ions, respectively. The coordination bond lengths of the Fe^{III} ions are 1.906(4) - 1.934(4) for the Fe-C bonds and 1.951(3) - 1.990(3) for the Fe-N bonds, which are characteristic of LS Fe(III) ions. The nickel(II) ion has a distorted octahedral coordination structure with four nitrogen atoms from (*R*)-pabn and two cyanide nitrogen atoms in the *cis* positions.

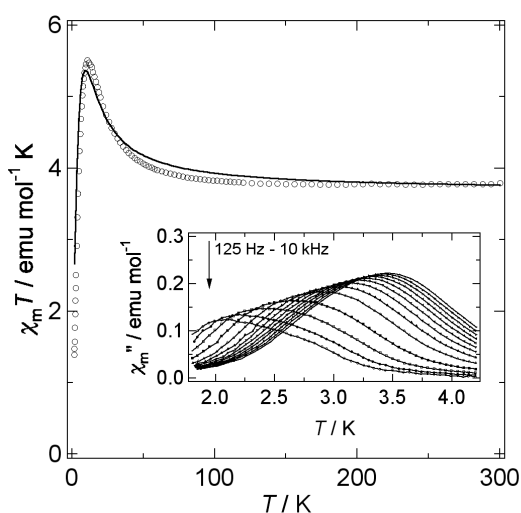


Fig. 2 $\chi_m T$ versus T and χ_m'' versus T plots (inset) for **1**. The solid line was calculated using the parameters given in the text.

Magnetic susceptibility measurements for powdered samples of **1** and **2** were performed in the temperature range of 1.8 - 300 K under an external magnetic field of 0.05 T (Figure 2 and 3). The $\chi_m T$ value of **1** is 3.78 emu mol⁻¹ K at 300 K, which is close to the value (3.74 emu mol⁻¹ K) expected for the two uncorrelated iron(III) ($S = 1/2$) and two nickel(II) ($S = 1$) ions, supposing the g_{iso} value of 2.33. Note that cyanide bridged Fe^{III}-Ni^{II} clusters have shown relatively large g_{iso} values ranging from 2.29 to 2.67.¹⁰ As the temperature was lowered, the $\chi_m T$ values gradually increased and reached the maximum $\chi_m T$ value of 5.50 emu mol⁻¹ K at 11 K, suggesting the occurrence of intramolecular

ferromagnetic interactions. The sudden decrease of the $\chi_m T$ values below 11 K is due to magnetic anisotropy and/or intermolecular antiferromagnetic interactions. Magnetic susceptibility data were analysed by Heisenberg spin Hamiltonian with an anisotropic D value for the lowest $S = 3$ state;

$$\hat{H}_{\text{HDVV}} = -2J \left(\hat{s}_4 \cdot \hat{s}_1 + \sum_{i=1}^4 \hat{s}_i \cdot \hat{s}_{i+1} \right) - g\beta\mu_0 H \cdot \sum_{i=1}^4 \hat{s}_i - D \left[\hat{S}_z^2 - 1/3 S(S+1) \right] - 2zJ' S \langle S \rangle$$

where J is the exchange coupling constant between iron(III) and nickel(II) ions and g is the average Landé g factor, and the intermolecular antiferromagnetic interaction was included by using the mean field correction. The best fitting parameters obtained are $g = 2.31(1)$, $J = 2.2(1)$ cm⁻¹, $D = -3(1)$ cm⁻¹, and $zJ' = -0.05(1)$ cm⁻¹. The pyrazole groups, coordinating to iron ions, in the neighboring molecules have close contact with the interplane distance of 3.22 Å, and this might be responsible for the intermolecular interactions. Note that high-field epr measurements at 5 K gave no absorption peaks. The occurrence of the intramolecular ferromagnetic interactions can be understood by the orthogonal magnetic orbitals of dπ and dσ spins on the low-spin Fe(III) and the high-spin Ni(II) ions, respectively. AC magnetic susceptibility measurements for a powder sample of **1** were performed in the temperature range of 1.8 - 4.2 K with oscillating field of 3 G (Figure 2, inset). Both in- and out-of phase signals showed frequency dependence and their peak maxima moved to lower temperatures as the AC frequency was lowered. Noted that the out-of-phase signals consist of two components. The Arrhenius plot, assuming that the relaxation time (τ) at the peak-top temperature of χ'' was well approximated by the inverse of the AC frequency, can be analysed by two lines in the temperature ranges of 2.00 - 2.67 K and 2.90 - 3.45 K (Figure S1). Least square calculations gave effective energy barriers (ΔE) for magnetization reversal of 29.0(4) and 20.3(3) K with the pre-exponential factors (τ_0) of $2.3(3) \times 10^{-8}$ and $4.7(9) \times 10^{-7}$ s for low and high temperature regions, respectively. The values are characteristic of SMMs, although the origin of the two components remains unclear.

The $\chi_m T$ value for **2** is 2.14 emu mol⁻¹ K at 300 K which is larger than the value (1.375 emu mol⁻¹ K with $g = 2.0$) expected for the uncorrelated LS Fe(III) ($s = 1/2$) and Ni(II) ($s = 1$) ions and this is due to the large g_{iso} value. The $\chi_m T$ values for **2** increased slightly as the temperature was lowered, and showed sudden increase at 40 K, reaching the maximum value of 51.9 emu K mol⁻¹ at 3.5 K, before decreasing rapidly. The temperature dependence of the $\chi_m T$ values suggests the occurrence of intrachain ferromagnetic interactions which are due to orthogonal magnetic orbitals of the LS Fe(III) and Ni(II) ions. Magnetic susceptibility data were analysed using a high-temperature model for Heisenberg ferromagnets.¹¹ The zero field magnetic susceptibility is formally expanded in a power-series of the variable J/kT and is expressed as:

$$\chi_M = (C/T) \left\{ 1 + \sum_{n=1} A_n (J/kT)^n \right\}$$

$$C = \left(\frac{Ng^2\mu_B^2}{3k} \right) \{ S_{Fe}(S_{Fe} + 1) + S_{Ni}(S_{Ni} + 1) \}$$

where k is Boltzmann's constant, C is the Curie constant, and A represents the coefficients in the series.¹¹ Least square calculations yielded the J value of 6.4(1) cm⁻¹ with $g = 2.40(1)$.

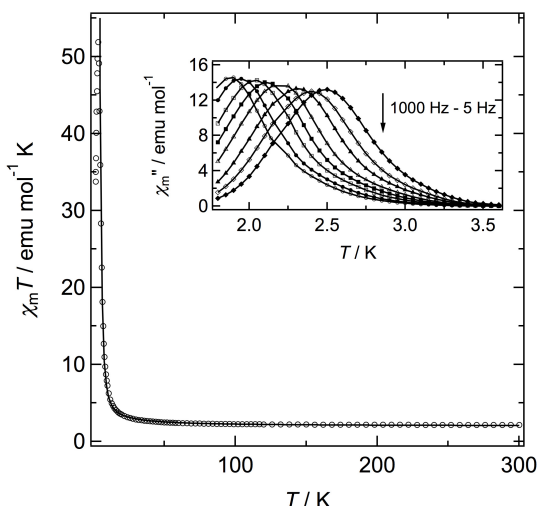


Fig. 3 $\chi_m T$ versus T and χ_m'' versus T plots (inset) for **2**.

AC magnetic susceptibility measurements for a powder sample of **2** were performed in the temperature range of 1.8 – 3.6 K with oscillating field of 3 G (Figure 3, inset), and both in- and out-of phase signals displayed frequency dependence, confirming the existence of slow magnetic reorientation. The Arrhenius plot gave an effective energy barrier for magnetization reversal $\Delta E = 40.4(3)$ K and a pre-exponential factor $\tau_0 = 9(2) \times 10^{-11}$ s, with the latter particularly characteristic of a SCM. A Cole-Cole plot was analysed by the generalized Debye model (Figure S2), and the α value of 0.35 was obtained at 2.1 K, suggesting monodispersibility of magnetization relaxation at 2.1 K.¹² In summary, a chiral SCM and achiral SMM were isolated by using optically pure and a racemic mixture of ligands as starting materials, respectively.

This work was supported by a Grant-in-Aid for Scientific Research and for Priority Area "Coordination Programming" (area 2107) from MEXT, Japan.

Notes and references

- † [Fe^{III}₂Ni^{II}₂(CN)₆(tp)₂[(*R*)-pabn][(S)-pabn]](PF₆)₂·H₂O·4CH₃CN (**1**): Racemic mixture of pabn (23.3 mg, 0.05 mmol) in acetonitrile (1 cm³) was added to NiCl₂·6H₂O (10.9 mg, 0.05 mmol) in acetonitrile (1 cm³). After stirring for an hour, (Bu₄N)[Fe(CN)₃(tp)] (29.5 mg, 0.05 mmol) and Bu₄NPF₆ (19.4 mg, 0.05 mmol) in methanol (2 cm³) were added. After stand for a few days at 35 °C, brown needles of **1** (28.6 mg, 52 %) were obtained (Found: C, 51.60; H, 3.96; N, 18.28. Calc. for C₉₂H₈₀B₂F₁₂Fe₂N₂₈Ni₂O₁P₂: C, 51.77; H, 3.78; N, 18.37 %).
- catena-[Ni^{II}[(*R*)-pabn]][Fe^{III}(tp)(CN)₃]PF₆·2MeOH (**2**): **2** was obtained by the same manner as **1** by using the optical pure ligand of

(*R*)-pabn in methanol. Black rod crystals of **2** (10.8 mg, 20 %) were obtained (Found: C, 51.42; H, 3.76; N, 17.54. Calc. for C₄₅H₄₀B₁F₆Fe₁N₁₃Ni₁O₁P₁: C, 51.51; H, 3.84; N, 17.35 %).

§ Crystal data for **1**: C₉₆H₈₆B₂F₁₂Fe₂N₃₀Ni₂O₁P₂, $M = 2216.63$, triclinic, $a = 9.212(4)$, $b = 13.535(6)$, $c = 20.115(9)$ Å, $\alpha = 101.840(6)$, $\beta = 92.846(6)$, $\gamma = 100.063(6)$ °, $V = 2407(2)$ Å³, $T = 93(2)$ K, space group $P\bar{1}$ (no. 2), $Z = 1$, 9735 reflections measured, 7406 unique ($R_{\text{int}} = 0.0630$) which were used in all calculations. The final $R1$ and $wR2$ were 0.085 and 0.202 ($I > 2\sigma(I)$).

Crystal data for **2**: C₄₆H₄₄BF₆FeN₁₃NiO₂P, $M = 1081.28$, orthorhombic, $a = 10.6762(9)$, $b = 17.543(2)$, $c = 25.176(2)$ Å, $V = 4715.2(7)$ Å³, $T = 100(2)$ K, space group $P2_12_12_1$ (no. 19), $Z = 4$, 53177 reflections measured, 10307 unique ($R_{\text{int}} = 0.0731$) which were used in all calculations. The final $R1$ and $wR2$ were 0.048 and 0.105 ($I > 2\sigma(I)$). The Flack parameter was 0.01(1). The intensity data were collected on a Bruker SMART APEX diffractometer with graphite-monochromated MoK α radiation ($\lambda = 0.71073$ Å). Empirical absorption corrections by SADABS (G.M. Sheldrick, 1994) were applied to the reflection data. Direct methods were used to solve the structure and to locate the heavy atoms using the SHELXTL-97 program package. The remaining atoms were found from successive full-matrix least-squares refinements on F^2 and Fourier syntheses.

- 1 Q.-H. Xia, H.-Q. Ge, C.-P. Ye, Z.-M. Liu and K.-X. Su, *Chem. Rev.*, 2005, **105**, 1603; G. Koeckelberghs, C. Samyn, A. Miura, S. De Feyter, F. C. De Schryver, S. Sioncke, T. Verbiest, G. De Schaezen and A. Persoons, *Adv. Mater.*, 2005, **17**, 708; R.P. Lemieux, *Acc. Chem. Res.*, 2001, **34**, 845; W. Eerenstein, N. D. Mathur and J. F. Scott, *Nature*, 2006, **442**, 759.
- 2 G. L. J. A. Rikken and E. Raupach, *Nature*, 1997, **390**, 493; C. Train, R. Gheorghe, V. Krstic, L.-M. Chamoreau, N. S. Ovanesyan, G. L. J. A. Rikken, M. Gruselle and M. Verdager, *Nat. Mater.*, 2008, **7**, 729.
- 3 (a) K. Inoue, K. Kikuchi, M. Ohba and H. Ōkawa, *Angew. Chem.*, 2003, **115**, 4958; *Angew. Chem., Int. Ed.*, 2003, **42**, 4810; (b) H. Imai, K. Inoue, K. Kikuchi, Y. Yoshida, M. Ito, T. Sunahara and S. Onaka, *Angew. Chem. Int. Ed.*, 2004, **43**, 5618; (c) E. Coronado, C. J. Gómez-García, A. Nuez, F. M. Romero and J. C. Waerenborgh, *Chem. Mater.*, 2006, **18**, 2670; (d) W. Kaneko, S. Kitagawa, M. Ohba, *J. Am. Chem. Soc.*, 2007, **129**, 248; (e) E. Coronado, J. R. Galán-Mascarós, C. J. Gómez-García and J. M. Martínez-Agudo, *Inorg. Chem.*, 2001, **40**, 113.
- 4 Y.-L. Bai, J. Tao, W. Wernsdorfer, O. Sato, R.-B. Huang and L.-S. Zheng, *J. Am. Chem. Soc.*, 2006, **128**, 16428.
- 5 L. Cavigli, R. Sessoli, M. Gurioli and L. Bogani, *Phys. Status Solidi A*, 2006, **203**, 1402.
- 6 G. Christou, D. Gatteschi, D. N. Hendrickson and R. Sessoli, *MRS Bull.*, 2000, **25**, 66; D. Gatteschi and R. Sessoli, *Angew. Chem., Int. Ed.*, 2003, **42**, 268; H. Oshio and M. Nakano, *Chem.-Eur. J.*, 2005, **11**, 5178.
- 7 C. Coulon, H. Miyasaka and R. Clérac, *Struct. Bond.*, 2006, **122**, 163.
- 8 H. Huang, T. Okuno, K. Tsuda, M. Yoshimura and M. Kitamura, *J. Am. Chem. Soc.*, 2006, **128**, 8716.
- 9 J. Kim, S. Han, I.-K. Cho, K. Y. Choi, M. Heu, S. Yoon and B. J. Suh, *Polyhedron*, 2004, **23**, 1333.
- 10 D. Li, R. Clérac, G. Wang, G. T. Yee and S. M. Holmes, *Eur. J. Inorg. Chem.*, 2007, 1341; W. Liu, C.-F. Wang, Y.-Z. Li, J.-L. Zuo and X.-Z. You, *Inorg. Chem.*, 2006, **45**, 10058; D. Li, R. Clérac, S. Parkin, G. Wang, G. T. Yee and S. M. Holmes, *Inorg. Chem.*, 2006, **45**, 5251.
- 11 P. J. Wojtowicz, *Phys. Rev.* 1967, **155**, 492; N. Fukushima, A. Honecker, S. Wessel and W. Brenig, *Phys. Rev. B*, 2004, **69**, 174430.
- 12 K. S. Cole and R. H. Cole, *J. Chem. Phys.*, 1941, **9**, 341.